HHS Public Access

Author manuscript

Expert Opin Drug Discov. Author manuscript; available in PMC 2016 December 01.

Published in final edited form as:

Expert Opin Drug Discov. 2015 December ; 10(12): 1347–1361. doi:10.1517/17460441.2015.1091814.

High throughput fluorescence imaging approaches for drug discovery using *in vitro* and *in vivo* three-dimensional models

Natalia J. Martinez[a,#], **Steven A. Titus**[a,#], **Amanda K. Wagner**[a,#], and **Anton Simeonov**[a,*]

[a]National Center for Advancing Translational Sciences, National Institutes of Health, Rockville, MD, 20850

Abstract

Introduction—High-resolution microscopy using fluorescent probes is a powerful tool to investigate individual cell structure and function, cell subpopulations, and mechanisms underlying cellular responses to drugs. Additionally, responses to drugs more closely resemble those seen *in vivo* when cells are physically connected in 3D systems (either 3D cell cultures or whole organisms), as opposed to traditional monolayer cultures. Combined, the use of imaging-based 3D models in the early stages of drug development has the potential to generate biologically relevant data that will increase the likelihood of success for drug candidates in human studies.

Areas covered—The authors discuss current methods for the culturing of cells in 3D as well as approaches for the imaging of whole-animal models and 3D cultures that are amenable to high throughput settings and could be implemented to support drug discovery campaigns. Furthermore, they provide critical considerations when discussing imaging these 3D systems for high throughput chemical screenings.

Expert opinion—Despite widespread understanding of the limitations imposed by the 2D *versus* the 3D cellular paradigm, imaging-based drug screening of 3D cellular models is still limited, with only a few screens found in the literature. Image acquisition in high throughput, accurate interpretation of fluorescent signal, and uptake of staining reagents can be challenging, as the samples are in essence large aggregates of cells. The authors recognize these shortcomings that need to be overcome before the field can accelerate the utilization of these technologies in large-scale chemical screens.

Keywords

3D cellular models; whole-animal imaging; fluorescent imaging; high content; high throughput screen; drug discovery

[*]Corresponding author (asimeono@mail.nih.gov).
[#]Equal contribution

Financial and Competing Interests Disclosure

The authors are employees of and are supported by the National Institutes of Health. The authors have no other relevant affiliations or financial involvement with any organization or entity with a financial interest in or financial conflict with the subject matter or materials discussed in the manuscript apart from those disclosed.

1. Introduction

1.1 3D cellular systems in drug screening campaigns

The academic and private sectors have invested massively in the area of high throughput screening (HTS) as a means to assess small molecule libraries in miniaturized assays to identify lead compounds with therapeutic potential. Traditionally, HTS has been limited to *in vitro* biochemical and two-dimensional (2D) cellular assays, with cells typically residing as a monolayer on the bottom of the well of a microtiter plate. Although conventional 2D assays are informative (for instance, reporting on a compound's cell permeability or toxicity), they fall short in recapitulating the complex microenvironment and cell-cell interactions of a tissue or organism. A growing body of evidence indicates that cells grown in monolayers lose some of their physiological properties and do not faithfully recapitulate drug responses. Although not the topic of discussion here, we direct the reader to the following references for comprehensive reviews discussing the differences between 2D and 3D biology [1–4]. It is generally accepted that drug screening campaigns would benefit from the use of more relevant biological models that better translate results to the *in vivo* scenario [5–10]. Additionally, the analysis demonstrating that phenotypic screening leads to a higher proportion of FDA-approved drugs compared to target-based screening has been a major driver of the renewed interest in finding evermore physiologically relevant models for chemical screening [11]. These models include three-dimensional (3D) cell cultures and small model organisms that can be cultured in multi-well plates and treated with chemical libraries. Recent advances in the establishment of robust 3D systems amenable for high throughput screening have elicited significant interest as demonstrated by an increased commercial activity around 3D-based technologies. Multiple companies now commercialize plates, scaffolds and tool-box reagents amenable for the establishment and screening of 3D cell cultures. Hardware and software for high throughput imaging of 3D systems is also fast evolving. Finally, companies now offer fee-for-service screening and profiling of chemical entities in 3D cellular models.

1.2 Fluorescence imaging of 3D systems

A number of assay readouts and detection methods have been applied to 3D cell cultures. Homogeneous cytotoxicity and cell viability assays that measure metabolic activity, such as tetrazolium and resazurin reduction assays, acid phosphatase activity, and cellular ATP levels or cell membrane integrity, are typically employed as endpoint assays with colorimetric, fluorescence, or luminescence-based readouts [12]. Some of these methods often require disassembly and termination of culture (i.e. cell lysis) for analysis. In addition, colorimetric conversion products have been noted to bind to extracellular matrix (ECM) [13]. Although sensitive and amenable for high throughput testing, these assays detect responses representing averaged cell population effects. Brightfield microscopy is also usually employed to track overall changes in structure size. Because microscopy-based imaging using fluorescent probes can provide in-depth information about individual cell structure, function, and relative location, as well as overall changes in the morphology and growth of the 3D structure, it is quickly becoming a standard readout method. Imaging also informs on sub-populations such as those that are resistant or sensitive to drug treatment, in many cases without the need to disrupt the structures under testing. Moreover, imaging of

both fixed (endpoint) and live cultures is feasible and amenable for multiplexing with endpoint functional assays, including metabolic/viability described above, invasive potential, and/or morphological changes. Nowadays, several techniques for 3D fluorescence microscopy acquisition are available, such as widefield, confocal and super resolution microscopy.

For small molecule screening using whole organisms, brightfield microscopy is commonly used to characterize morphological or behavioral changes upon compound treatment. Increasingly, however, fluorescence microscopy is utilized to monitor the injection or uptake of fluorescent dyes and the expression profile of reporter constructs in transgenic animals (i.e. expressed in specific organs or cell populations). Confocal microscopy is the most popular, given the thickness of the organisms. However, standard widefield microscopy at low objective magnification has also been used to increase throughput.

The visualization of 3D cellular structures in high throughput is nevertheless challenging and analysis is confounded by light scattering and absorption of the thick biological sample, the method employed to culture cells in 3D, lack of homogeneous cell labeling when using certain fluorescent sensors, the need to determine body orientation before whole-animal image analysis, and others. Another main challenge is the automation of acquisition and analysis of images with reasonable throughput.

1.3 High throughput imaging-based screening in 3D models

For the purpose of drug discovery, 3D systems need to be scalable to relatively high throughputs, fast, simple, reproducible and amenable to automation (compatible with the liquid handling robots, plate readers and imaging platforms currently adopted by most academic and private labs). Only a few 3D systems, generally those with relatively low levels of complexity and/or cost, possess those characteristics. For these reasons, microfluidic and certain chip-based methods will not be discussed here, even though these systems allow for controlled environmental modifications [14].

Translating an imaging assay from 2D into 3D can be quite difficult. Certain information obtainable from 2D systems is often not possible in 3D cultures or whole animals. For example, subcellular events such as nuclear translocation or vesicle trafficking are not resolvable in 3D models due to sample background and other physical constraints (see section 3.1). Therefore, 3D imaging screens are primarily suitable for macro-level readouts such as cellular identification or viability. Standard 2D procedures such as fixation and antibody staining involving multiple washes are not readily transferable, in particular to non-adherent 3D systems. Penetration of reagents into the 3D structure and potential volumetric collapse with fixation all must be empirically determined before the screen can begin.

We discuss in the next section the current 3D cellular systems amenable to high throughput imaging-based screens starting with *in vitro* 3D cell cultures followed by *in vivo* whole animal models. We highlight benefits and drawbacks of each methodology and provide examples when available. Current imaging strategies, including hardware and analysis methods are discussed in more detail in section 3.

2. 3D models amenable for imaging-based high throughput screening

2.1 *In vitro* 3D cell cultures

The term “3D culture” is ambiguous; herein, 3D cultures are those where cells aggregate with each other into 3D structures *via* cell-cell and cell-ECM interactions. A wide range of 3D cellular models have been developed, which can be applied to various research applications including toxicology, cancer, and stem cell drug discovery. These models can be either single (homotypic) or multi-cell-type (heterotypic). Each model has advantages and limitations, and, given the diverse requirements of different cell types and applications, not one specific 3D system is regarded as the “gold standard”. Despite their diversity, all provide structural and cellular morphological complexity that yields different responses to therapeutic compounds compared to traditional monolayer cultures. Excellent comprehensive reviews of 3D tissue models, especially those not yet amenable to early phases of drug discovery due to throughput limitations, such as self-assembled heterotypic organoid cultures, are found in references [15–17].

The most popular and commonly employed 3D models are single-cell type and mixed co-culture spheroids because of their relative ease and reproducibility of culture techniques, and the scalability to sustain high-throughput screens. Additionally, given appropriate matrix conditions and chemotactic cues, spheroid cultures can be modified to assess functionality, such as cell migration and invasion [18]. The main drawback of spheroids is the need to optimize size uniformity, important in order to standardize screen analysis. Spheroid size is critical because a concentric cell proliferation gradient is observed with proliferating cells in the periphery, cell-cycle arrested or dormant cells in the middle layers, and necrotic cells in the core, especially when spheroids reach ~500 μm in diameter [6].

2.1.1 Single cell-type spheroids—Single cell-type spheroids are typically self-assembled clusters of cells cultured in environments where cell-cell interactions dominate over cell-substrate interactions. In cancer drug screening, these spheroids are referred to as “multicellular tumor spheroids” as they mimic an avascular tumor nodule with regard to oxygen and nutrient gradients, ECM- and cell-cell contacts. Literature examples support the use of spheroids in oncology- and toxicology-oriented studies. These studies have demonstrated the superiority of spheroids over traditional monolayer cultures in terms of clinically relevant metabolic and proliferative responses to drugs, including chemoresistance [1,5,6,19]. Currently, efforts are directed at establishment of spheroid culture systems with induced pluripotent stem cell (iPSC)-derived material as well as patient-derived tumor cells to use in personalized medicine [20,21].

2.1.2 Mixed co-cultures—Mixed co-culture models better mimic the heterogeneous composition of a normal tissue or tumor where cell-cell interactions, cell-ECM interactions, and environmental cues influence the phenotypic outcomes typically seen *in vivo* [22]. Tumor cells grown in a mixed cell-type spheroid model display different drug sensitivity patterns than when grown in single cell-type 3D spheroids [23]. For drug discovery purposes, having different cell types in the same well also provides an internal control for potential drug toxicity. Besides spheroids, other co-culture systems in which multiple layers

of ECM and different cell types are seeded in the same well are sometimes considered as "3D cultures" since heterotypic cell-cell interactions and cell-ECM interactions are taking place. These relatively simple multilayered cultures have been employed for the screening of drugs that affect various biological processes including angiogenesis and ovarian cancer metastasis [24,25].

2.2 Current methods for 3D cell culturing

Several automation-friendly methods are currently available for 3D culturing. They can be categorized into scaffold-free or scaffold-dependent systems, in which cells are cultured without or in the presence of a natural or synthetic substrate for support or attachment, respectively (Figure 1). These methods typically allow one to optimize size and number of aggregates/well by adjusting the initial cell number and time of culture and are overall suitable for the culturing of single- and multi-cell type spheroids. In contrast to 2D, where cells can be cultured in ultra-throughput formats, current 3D cultures are limited to 96- and 384-well formats, allowing only focused-library or small-scale validation screens. Additionally, imaging of spheroids is heavily influenced by the method utilized to culture cells.

2.2.1 Scaffold-free methods—Among scaffold-free techniques (Table 1) we find the liquid overlay methods, which consist of culturing cells in non-adhesive surfaces like round bottom ultra-low attachment (ULA) [18,26], agarose-coated [27,28], or poly HEMA-coated plates [29,30]. A comparison of these methods concluded that spheroids grown in ULA or agarose-coated plates were reproducible in size and number of spheroids per well (1 spheroid/well) and display comparable growth curves, oxygen and nutrient gradients. The spheroids grown on ULA plates, however, showed more compact structures and grew to slightly larger sizes than those grown on agarose-coated plates, while spheroids grown in poly-HEMA-coated plates were non-reproducible in size [18]. The hanging drop technique, where spheroids are cultured in a hanging drop plate before being transferred to a separate plate for follow-up analysis, is another type of the liquid overlay method [31–34]. Magnetic levitation has also been used to set up 3D spheroids in scaffold-free conditions. In this method, cells are labeled with magnetic nanoparticles and upon application of a magnetic field, cells are brought together to interact and aggregate with each other to form larger 3D cultures [35]. Magnetic labeling has also been used for immobilization of spheroids to allow media changes while minimizing disruption [36]. The scaffold-free methods described above prevent cell attachment to the well surface and induce cell aggregation and the formation of uniform floating spheroids at the bottom of the well (or drop in the case of hanging drop plates). The extracellular matrix keeping spheroids together is naturally secreted by the cells. Most such methods are available in 96- and 384-well format and yield spheroids of homogenous sizes at a single aggregate per well. Since these methods rely on cells' ability to establish cell-cell contacts, however, certain cell types dissociate easily and do not form compact spheroids in these conditions [29]. To address this issue, Ong and colleagues reported the generation of scaffold-free, dense spheroids by connecting cells directly but transiently with an inter-cellular linker that facilitates aggregation [37]. Due to their "floating" nature, spheroids generated by liquid overlay methods often pose autofocus challenges when imaging.

Liquid overlay methods are well suited for co-cultures, mostly when different cell-types are mixed prior to seeding for 3D growth. Co-cultures of hepatocyte spheroids and stromal cells (such as fibroblasts or nonparenchymal cells) are now commercially available in 96-well format for toxicology applications (InSphero). Liquid overlay methods also allow the sequential addition of various cell types, resulting in layered spheroids that are, for instance, suitable for the study of cell migration and invasion in 3D. Indeed, co-culture spheroids with randomly-distributed as well as patterned concentric layers cells of different types formed using hanging drop and ULA plates have been described [32,38–40]. For example, Ivanov *et al.* reported a spheroid co-culture of differentially labeled normal human fetal brain tissue and medulloblastoma tumor cells [39]. The spheroids adopted a polarized shape with discrete tumor cells-dominated and normal cells-dominated regions.

2.2.2 Scaffold-dependent methods—Other methods use scaffolds to seed cells close together to promote aggregation (Table 1). Scaffold-dependent methods include growing spheres on top of substrates coated with ECM-based preparations (such as collagen or Matrigel) and/or biologically inert organic matrices, such as agar [30,41]. A similar principle is used in patterned plates in which nanoscale rectangular grid patterns are printed on transparent synthetic-resinous bases or ECM-coated plates to provide a scaffold to which cultured cells can aggregate to form spheroids [21,42]. The utility of these micropatterned plates for drug screening was recently demonstrated using patient-derived spheroids in a 96-well format [21]. Co-cultures of hepatocyte spheroids and stromal cells have also been reported using micropatterned techniques [43,44]. Because growing spheres on top of substrates allows their attachment to the bottom of the well, these methods are better suited for imaging than spheroids in suspension. However, optical aberrations could arise due to light scattering/absorption by the scaffold or uneven scaffold surfaces. Scaffold-dependent protocols also include seeding cells fully embedded in the substrate and allowing them to form spheroids. For example, co-cultures of tumor and mesenchymal stem cells embedded in ECMs have been reported [45]. In contrast to the methods described above, embedding cells in the substrate makes it harder to control the number and size of spheroids per well [46–48]. Other inert scaffolds, such as chemically defined hydrogels and alginates, allow the modulation of stiffness to mimic the stiffness of a particular tissue [49–51]. The inert degradation of the gel at the end of the culture period allows the isolation of live cells for further downstream processing and imaging. However, imaging of spheroids within the scaffold has not been assessed. It is likely that the image quality of scaffold-embedded spheroids might be compromised due to optical aberrations and intensity attenuation produced by the scaffold. Accordingly, Reid *et al.* implemented an imaging protocol in which tumor spheroids grown in agarose and Matrigel coated plates were transferred to 96-well plates containing media before imaging [52]; adding such a transfer step, however, places a natural burden on the protocol. Overall, the possibility of certain scaffolds interfering with microscopy imaging should be considered and, in the case of scaffold-embedded spheroids, differential drug penetration could pose another issue. In addition, dispensing of certain scaffolds into micro-well plates requires special handling, which poses a challenge for automation. For example, Matrigel and agarose should be dispensed at low and high temperatures, respectively, to prevent solidification before reaching the well.

2.3 Whole model organisms

The nematode *Caenorhabditis elegans* and the zebrafish *Danio rerio* are among the most attractive animal models for drug discovery based on low cost and culture conditions compatible with large scale screens. Importantly, these organisms are genetically tractable, have well-defined developmental stages, and are transparent, facilitating imaging-based screens. Using them as models has provided insights into the molecular and cellular basis of human disease because approximately 50% and 70% of *C. elegans'* and *D. rerio*'s genes, respectively, have a human counterpart. However, whole organisms pose a challenge for fluorescence-based high-throughput screening. Not only are the physical limits of light microscopy important considerations, as for 3D cell cultures, but practical problems of distributing embryos and larvae into multi-well plates, the need of immobilizing animals before imaging, and setting up analysis algorithms that can identify and adjust to asymmetrical body plans in the final image, make this a challenging field. With these difficulties, whole organism screening has primarily been limited to low- and medium-throughput assays. Nevertheless, several labs have come up with creative solutions for some of the above problems and industry is beginning to follow up with commercial equipment to address their needs. As a result, screens for toxicity, mutagenesis, cell migration, and proliferation in whole organisms are now a reality.

Below we outline the various methods devised to address the above issues in the fluorescent screening of immobilized *D. rerio* and *C. elegans* models. Of note, many groups are working on screening for drugs affecting the cardiovascular system of zebrafish without immobilizing them first. Necessarily, this is done using live video feeds and corresponding tracking analysis. We will not cover this work in detail here, but refer interested readers to papers such as [53–55].

2.3.1 Zebrafish (*Danio rerio*)—The optical transparency of zebrafish embryos and larvae allows the *in vivo* observation of fluorescent probes and/or morphological defects as readouts in a chemical screen. Zebrafish embryos develop externally and relatively quickly, with most internal organs and systems functioning in the first 24–48 hours post fertilization, and large numbers of embryos can be obtained [8]. Organ and disease development can be modeled in zebrafish. The majority of screens thus far have been somewhat limited in their size due to the need for plating animals manually. Several groups report handling embryos and larvae automatically without harming them. Pardo-Martin *et al.* designed a custom fluidics system that leaves larvae sufficiently unharmed that they survive well and can be imaged over multiple days [56]. This method does require a complex setup, however, and will require further development before it is practical for widespread usage. By customizing the commercially available COPAS Biosort XL (now called FP-2000), Letamendia *et al.* automatically dispensed embryos of the same age based on their size. They observed no difference in heart rate, morphology or development between embryos dispensed automatically or manually, making this an attractive option for labs seeking to work on larger scale zebrafish screens [53].

Most zebrafish chemical screens require the immobilization of embryos/larvae through anesthetics and/or by plating them in agarose, in order to achieve acceptable image

resolution. For example, Gehrig *et al.* plated embryos in 96-well agarose-embedded plates and manually oriented them. Without manipulation, the orientation of each animal can vary within wells, necessitating an extra image analysis step designed to locate the pertinent region of the fish (i.e. head) [56–59]. Vogt *et al.* looked at tail blood vessel morphology to assess cardiovascular development and defects in transgenic fluorescent embryos. Entire wells were imaged by using low magnification in 96-well plates. For this work, however, results from embryos that were not in the optimal orientation had to be eliminated because the software could not accommodate the variations [57]. After developing in-house software based on Matlab, Peravali *et al.* quantified data from all embryos regardless of orientation to map monoaminergic neurons in GFP transgenic animals [58].

Overall, analyses now either accommodate the need to identify gross morphological areas of an animal or avoid the need to do so in its entirety. A remaining challenge is the plating of organisms automatically: for the time being, zebrafish are best suited to follow-up assays, for example measuring toxicity effects that would not be noticeable in a spheroid model (such as cardiovascular or neurological development, or subtle effects of toxicity).

2.3.2 Nematode (Caenorhabditis elegans)—*C. elegans* is widely used to model many molecular disorders but, due to its distance from mammals in the evolutionary tree, some diseases cannot be reproduced. When appropriate, however, its small size, optical transparency, short life cycle, simple growth conditions, and low-cost make it an excellent choice for large-scale screens [60].

The smaller size of *C. elegans* has enabled researchers to adopt automated dispensing more easily than with zebrafish. Many groups are also using the COPAS Biosorters and a group has developed a method to seed worms using a standard peristaltic pump [9,61–64]. Much of the groundwork has been laid even for density titrations down to 384-well plates. The animals, however, must still be synchronized in developmental stage before screening can be done or the analysis needs to distinguish animal age by size or another metric. In general, *C. elegans* also needs to be immobilized before imaging. However, at least one group has used the nematodes' natural motility as an asset for toxicity readouts [64].

Further difficulties with screening in *C. elegans* include dosing in the small molecules, which are typically impermeable through *C. elegans* cuticle and may be potentially broken down by the *E. coli* present with the worms [9]. Additionally, as in other systems, the 3D images generated are in general too cumbersome for standard analysis algorithms to process and must be flattened to 2D prior to analysis. As in zebrafish, imaging readouts for *C. elegans* need to be mapped to the appropriate body region before analysis can be done (*i.e.*, locate head before neurons can be found). However, the ease of making transgenics in *C. elegans* makes adding region-specific tags an approachable task. As methods and equipment continue to improve, *C. elegans* will become even more attractive for use in truly high-throughput whole organism screening.

2.4 Fluorescent sensors

Fluorescent sensors, such as small molecule dyes commonly applied to the imaging of cell monolayers, have been adapted and are frequently used to image spheroids [18,29]. As in

2D, most of these sensors are incubated with the spheroids right before detection and used to image fixed or live samples. Common readouts include cell viability, mitochondrial membrane potential/integrity, GPCR and ion channel activity, and hypoxia. These assays are performed with a variety of fluorescent dyes such as: for viability (i.e. calcein-AM, propidium iodide, CyQUANT, Hoechst 33342, EthD-1, SYTOX Green), mitochondrial membrane potential and integrity (i.e. TMRM, JC10, MitoTracker, MitoView), GPCR/channel activity (Fluo-4, Fura-2 and related dyes), hypoxia (i.e. CYTO-ID, HypoxiSense 680, LOX-1), to name but a few. For a recent review of small molecule fluorescent dyes, please see [65].

Immunostaining of fixed spheroids with specific fluorescent antibodies is also commonly employed. For instance, anti-pimodinazole antibodies are used to mark hypoxic regions in spheroids [66]. However, protocols involving multiple washing steps are not preferable in high throughput settings. In contrast to single cell type systems, co-cultures require the differential labeling of cells. A common strategy is the use of fluorescent dyes such as CellTrackers (Life Technologies), which are taken up by cells prior to 3D culturing and chemical exposure. Examples of this strategy are found in references [32,39,67]. However, the sensor's signal diminishes after each cell doubling so they are only useful for relatively short term cultures. The main advantage of fluorescent dyes is that they allow the labeling of virtually any cell type, including patient-derived cells.

Engineered cell lines that express a fluorescent gene reporter have also been used [18,32,33,38,42,48,52,68]. For example, Reid *et al.* utilized a GFP reporter to track a subpopulation of cancer stem cells existing within a population of luminal breast cancer cells [52]. Genetically encoded sensors do not suffer from differential bioavailability and penetration issues as certain fluorescent dyes (see section 5). In addition, a physiologically relevant and uniform cell-to cell-expression can be achieved especially when stable cell lines are generated by genome editing technologies. Genetically encoded sensors provide a signal that is stable over time but are only useful when working with cell lines, which need to be engineered to express the fluorescent protein of interest prior to 3D culturing and are frequently time intensive to build [38].

Most fluorescent screens in zebrafish have utilized either transgenic lines or have a reporter construct or dye microinjected directly into the animals at early stages [8,57–59,69–71]. Gehrig *et al.* microinjected embryos with an array of fluorescent reporter constructs to map the interaction between cis-regulatory elements and core promoters [59]. A multi-fluorescent label zebrafish line was developed by Tsuji *et al.* to build an *in vivo* sensor for beta-cell activation and proliferation in the pancreas [72]. Finally, an *in vivo* screen for compounds that prevent metastasis of cancer cells was performed by Gallardo *et al.* Zebrafish embryos expressing a fluorescent tag in the postlateral line primordium were used to screen for compounds that prevent the delamination and migration of these cells. Importantly, hits from the initial screen were further tested in a murine tumor model and found to be effective, affirming the applicability of this system for future work [70]. As with spheroid cultures, genetically encoded sensors can achieve uniform expression and specific labeling of populations without the need for individual microinjections. However, this must be balanced with the effort necessary to generate a stable line.

Transgenic fluorescent lines are also commonly used in *C. elegans* [62,73]. Maglioni *et al.* have investigated mitochondrial stress as shown by gross morphology and fluorescence activation of heat shock proteins [73]. Uptake of fluorescent dyes in *C. elegans* is a useful alternative to creating transgenic lines [61,64]. Thus far, researchers have used primarily live dyes to fluorescently label only the dead worms due to significant challenges with dye penetration in intact worms [60,74]. One of the most comprehensive investigations into using *C. elegans* for screening came from Gosai *et al.* The authors imaged worms in 96- or 384-well plates. Animals were categorized based on size, and neurons and autophagosome spots were detected to distinguish phenotypes and dead animals were identified *via* SYTOX green uptake [61]. Moy *et al.* automatically dispensed animals into 384-well plates and performed a toxicity screen using SYTOX Orange to label dead worms in a screen for novel antibiotics [64].

3. Methods for high throughput imaging and analysis of 3D cellular models

3.1 Microscopy methods and hardware

The size of 3D cellular models such as spheroids and whole organisms can exceed several hundred μm in thickness and hence pose extra challenges to conventional fluorescence microscopy techniques normally applied to 2D cell cultures. Many commercially available imaging systems, both confocal and widefield, are capable of acquiring image stacks with defined optical Z plane sections.

Widefield fluorescence microscopy captures image sections that have a depth equivalent to the objective lens' respective depth of field. For example, a 20x 0.4 Numerical Aperture (NA) lens has a depth of field which is approximately 5.8 μm deep (for a review see reference [75]. This means that when imaging a sample several hundred μm thick, one can image sections ~6 μm at a time using a standard 20x 0.4 NA lens. In order to image an entire 300 μm sample, one would need to image 50 sections (or ~120 sections if using Nyquists sampling) to accurately capture the sample in its entirety. In the case of a 20x 0.4 NA lens, objects smaller than 5.8 μm would all appear in the same focal plane and could appear as slightly fuzzy or out of focus. Deconvolution, or image processing of 3D images, utilizes mathematical formulas based on the objective lens and optical properties of the imaging system to essentially restore out-of-focus light back to its original point source. This, in turn, can produce images with much higher contrast than standard widefield counterparts (Figure 2). Confocal microscopy, on the other hand, utilizes an electronic or mechanical hardware that blocks out of focus light at a defined depth *via* a fixed size slit, pinhole, or electronic shutter. In the case of confocal microscopy, optical thickness is determined by the objective lens's NA as well as the size of the shutter (pinhole, slit, etc.).

While both widefield and confocal microscopy have resolution limits based on the refraction limits of light (around 250 nm minimum), super-resolution microscopy methods can resolve objects approaching 10 nm or less [76,77]. Emerging imaging methods such as Light Sheet Fluorescence Microscopy (LSFM), Structured Illumination (3D SIM), and Multiphoton Microscopy hold great promise for deeper sample penetration and have been recently employed to image whole animals, spheroids and tissue sections [78–81]. These methods require expensive instrumentation and specialized sample preparations that are typically not

suitable for automated imaging campaigns. For an excellent overall review and guide on fluorescence microscopy methods, see references [82] and [83].

Each imaging modality has its strengths and weaknesses (Table 2). Generally, as image resolution increases, acquisition speed (and throughput) decreases and cost increases. Widefield systems are the least costly but cannot typically penetrate deeper than a few cellular layers in a spheroid [18]. Deconvolution can increase image contrast and resolution; however, not all deconvolution algorithms are truly quantitative so one must exercise caution when analyzing deconvolved images. For a comprehensive review on image deconvolution algorithms see [82].

Stand-alone fluorescence microscopes can be fitted with X, Y, and Z motors and autofocus modules for higher throughput applications but the additional cost often shifts the decision towards purchasing dedicated high content instruments, which are typically more robust with intensive usage. There are commercially available choices for high content instruments ranging from whole-well imagers to high magnification systems, which use widefield and confocal modalities (Table 3). Recent advances in instrument hardware such as in light (solid state illumination, solid state lasers) and camera technology (scientific grade large format CMOS cameras) have resulted in many high speed, relatively low-cost imagers capable of reading a 384-well plate in 5 minutes or less. Because many confocal systems physically block out of focus light with a slit or pinhole, 80–90% of the total excitation light is also blocked resulting in dimmer emission signal. High-power light sources such as solid state illuminators or lasers are the best choice when combined with confocal imaging. When using high power light sources, issues such as phototoxicity and photobleaching must be considered, particularly when imaging multiple Z sections. Instruments that utilize super-resolution microscopy typically use immersion objectives for single sample imaging and are not currently amenable to multi-well high throughput screening campaigns.

3.2 Image analysis software

There are many options for image analysis, although those targeted to volumetric analysis of high-throughput 3D images are quite limited. There are many commercial programs available for 2D analyses, such as maximum projections and Z stacks, including software from GE, TTP LabTech, PerkinElmer, Life Technologies, Essen and others, generally intended for use with the corresponding machine, although many of these work across multiple platforms. They are good at handling the large datasets generated by screening, and several can calculate image parameters based on a maximum projection of a Z-stack as well as individual Z sections. TTP LabTech's software can conduct basic analysis of 3D spheroids natively [24], but highly detailed image data analysis is not possible with their software. There are only a few commercially available software packages with solutions for 3D rendering and volumetric analysis, primarily those from companies such as PerkinElmer (Volocity), Bitplane (Imaris) and Arivis Vision (Arivis 4D); however, these software packages can be cost prohibitive to smaller labs. Each system can calculate distances between structures in a 3D object as well as map connections, but only Volocity is able to handle large batch analyses of the types that would be generated by screening. Imaris and Arivis 4D seem to be geared more towards in-depth analysis of smaller batches of images.

All three systems recommend utilizing a multi-processor computing system for analysis of large batches and can be configured so that the work can be sent to a centralized server.

Several open-source methods for image analysis are becoming more popular. In particular, ImageJ and Fiji are appealing due to their flexibility and ever growing library of user-designed plugins. Fiji can be used to reconstruct 3D images from *C. elegans*, including computing intensive series such as long-term time-lapse images of development [84]. However, users often need to design an interface to accommodate the multiple well meta-data necessary to analyze multi-well plates. CellProfiler was designed specifically to handle large datasets from automation and screening, and can work with both images and flow cytometry data; it is based on a building-block style workflow and is highly flexible. However, it targets mainly 2D culture analysis and any 3D imaging would either need to be based on maximum projections or be programmed by the end user [85]. Phaedra and OMERO are two other open-source software programs that are used for image analysis and data management in large-scale screening datasets [86–89]. They can both import and analyze file types in a wide variety of common formats. OMERO was designed as a stand-alone data visualization, analysis, and management system to run within the Open Microscopy Environment and currently supports over 140 image file formats [87–89]. Phaedra can also support analysis of both imaging and flow cytometry data [86]. However, both OMERO and Phaedra were designed primarily for analysis of 2D data, so 3D images must either be flattened (e.g., maximally projected) or specific programming designed to take volume into account would need to be developed by the end user. A tool designed to calculate properties from a Z-stack maximum projection, but which can readily handle the large datasets generated by screening, was developed in Di *et al*. The authors developed the tool based on ImageJ to analyze both nuclei and another parameter. In this case, F-actin morphology and branching patterns were analyzed in several breast cancer cell lines grown in spheroid culture. This more in-depth analysis requires some upfront user investment to define parameters of interest and train the software, with the algorithm then identifying features of interest for the remainder of the screen [90].

Several open-source analysis tools for nuclear structure in 3D have recently been developed. Among them, TANGO is based on ImageJ and R, and runs off of Z-stacks [91]. Another tool is based on the Insight Segmentation and Registration and the Visualization Toolkits. This program is dedicated to correctly partitioning individual nuclei within a dense 3D matrix [92]. V3D is another open-source software; however, it stands out in that it was specifically designed for 3D image analysis of structures within an organism or cell properties within a structure. It is capable of handling extremely large images with the computing power of a standard computer, and does not require a 2D-reconstructed image to pinpoint a specific place in a 3D image. However, it is mostly designed for datasets comprised of a few large images rather than what would typically be generated by screening and renders the images based on a maximum projection of Z-stacks, but is amenable to user modification [93].

4. Conclusion

The demand for more physiologically relevant models, which can better recapitulate *in vivo* drug responses, has prompted advances in the implementation and characterization of

imaging-based 3D cell culture and whole-organism assays, as well as their optimization for high throughput screening. These advances have further been made possible by convergence in diverse technologies ranging from biomedical engineering to advanced optics. This is reflected in the increasing number of publications on 3D cellular models as well as the commercial launching of reagents and platforms for the culturing and imaging of 3D structures. Despite all these advances, the use of 3D systems in drug discovery programs is still limited to follow up studies.

5. Expert Opinion

Before we can see the widespread adoption of 3D systems by the scientific community for the screening of large compound libraries, many conceptual and practical restrictions need to be overcome. Conceptually, data generated using these methods still need to be validated against established *in vivo* models. Particularly for 3D cellular models, which are relatively new, further optimization of the models is likely going to be needed, including the incorporation of vascular components of tissues or extension of culture time for long-term drug studies. Related emerging efforts in the direction of increasing complexity in 3D include tissue printing (also referred to as bioprinting) and organs-on-chips (also referred to as tissue-chip or microphysiological systems); however, these platforms represent a departure from the microtiter plate-based format and are naturally better suited for testing of small number of compounds at the post-screen stages of a project.

Great strides have been made to establish innovative ways of culturing cells in 3D and to miniaturize cultures for high throughput testing. However, standardized protocols for the imaging of 3D structures are still lacking. Issues such as incubation time and penetration efficiency of fluorescent sensors into the 3D structure also need to be addressed. Since most fluorescent sensors have been developed for 2D cultures it is necessary to optimize them in 3D structures as noted in a study by Beauchamp *et al.* of spheroids made of iPSC-derived cardiomyocytes for cytosolic calcium signals using fluo-4 as a calcium-sensitive fluorescent probe where the calcium indicator only partially penetrated into spheres as shown by optical sections of the spheroids [34]. Wenzel *et al.* stained spheroids with the fluorescent dyes Hoechst 33342 (which stains nuclei of live/fixed cells) and SYTOX Green (which stains nuclei of dead cells) [28] and noted that these dyes have sufficient penetration into spheroids but that they required a 24-hour incubation prior to imaging, and dyes such as Hoechst can exhibit cytotoxicity and/or cell cycle arrest after prolonged treatment. The recent work by Bonnier *et al.* indicates that common dyes applied in 2D assays display differential diffusion and bioavailability when cells are grown in 3D collagen matrices, highlighting the importance of protocol adaptation to individual culture conditions [94]. Additionally, certain dyes could be differentially metabolized or transported out of the cell under 3D culture conditions: the commonly used cell viability dye calcein-AM is a known substrate of MDR transporters, which reportedly are upregulated in certain 3D culture settings compared to monolayers [95]. Finally, some sensors like near-infrared reagents (see below) have been noted to reach maximum signal intensity only 72 hour after spheroid staining. Nevertheless, it is worth mentioning current efforts aimed at improving imaging of 3D structures. To minimize the effect of light scattering, both private and academic groups have developed near infrared reagents [96] which contain dyes emitting at ~700 nm, a region where light

absorption and scattering of biological tissues is at a minimum. Furthermore, to enhance detection depth of 3D samples, several protocols and reagents, such as 3DISCO, CLARITY and Sca*l*e have been developed for the optical clearing of biological samples [97–99]. Aqueous fixative reagents such as Sca*l*e (PerkinElmer) for spheroid culture applications have also been released. A recent study implemented several optical clearing protocols for the imaging of scaffold-free spheroids of neuronal origin, including Clear(T2), Sca*l*e and SeeDB [100].

While there have been many microscopy based hardware improvements in speed and sensitivity, certain issues still remain. Images collected during acquisition, particularly image Z stacks, can generate large data files, on the order of 100s of GBs to TBs (on a daily basis), therefore large data storage drives are required. The data and storage drives must be backed up and archived, and this usually requires dedicated IT personnel. Other issues that occur during automated imaging such as autofocus errors (particularly with round bottom and micro patterned plates), slow acquisition times (due to Z stacks or imaging multiple fields of view), and phototoxicity induced by long exposures to dim samples are other examples that need to be addressed.

No imaging platform or software analysis package is currently regarded as the “gold standard”; several considerations need to be taken into account when choosing the best approach for a given assay, including resolution needed, imaging speed, computational time, throughput, need for custom algorithms, types of analyses required, and the need for volumetric calculations or interconnection mapping (Figure 3). Studies with whole animals illustrate this point. For example, Gehrig *et al.* microinjected zebrafish embryos with over 200 different fluorescent reporters to investigate the expression pattern of each reporter. The authors took small Z-stacks of each embryo at low magnification using a stand-alone microscope-based imaging platform (scan^R, Olympus), then a custom designed software warped the 3D images onto a 2D maximum projection of an ideal fish embryo for fluorescent expression analysis. This approach allowed the authors to minimize computational time while addressing expression down to the tissue level in the animals [59]. Lin *et al.* reported a study on heavy metal toxicity in zebrafish using transgenic lines that report on expression of heat shock proteins. By using commercially available whole-well imagers, the authors eliminated the need for animal orientation-algorithms to begin analysis, allowing for commercial software or standard ImageJ to be used [69]. A high-throughput pace of screening in zebrafish and *C. elegans* has been achieved by using fluorescent plate-reading technology [62,63]. The information from this type of screen is unquestionably valuable; however, by definition it sacrifices the ability to obtain actual images of the animals and cannot achieve the resolution possible with whole-well or microscopy readers. It is perhaps better suited for detecting fluorescent reporter activation or simple toxicity studies, rather than the more intricate systemic effects possible to interrogate when, for instance, specific cell migration, individual vasculature or other direct cell morphology data are available.

Despite the current conceptual and practical challenges we discussed above, we anticipate that the fast pace of innovation in the field of 3D biology and fluorescent imaging and their

integration into high throughput platforms for drug screening will likely facilitate the identification and validation of new therapeutics in the near future.

Bibliography

1. Abbott A. Cell culture: Biology's new dimension. Nature. 2003; 424:870–2. [PubMed: 12931155]
2. Weigelt B, Ghajar CM, Bissell MJ. The need for complex 3d culture models to unravel novel pathways and identify accurate biomarkers in breast cancer. Adv Drug Deliv Rev. 2014; 69–70:42–51.
3*. Pampaloni F, Reynaud EG, Stelzer EH. The third dimension bridges the gap between cell culture and live tissue. Nat Rev Mol Cell Biol. 2007; 8:839–45. Review discusses biological potential and applicability of 3D models. [PubMed: 17684528]
4. Mazzoleni G, Di Lorenzo D, Steimberg N. Modelling tissues in 3d: The next future of pharmaco-toxicology and food research? Genes Nutr. 2009; 4:13–22. [PubMed: 19104883]
5. LaBarbera DV, Reid BG, Yoo BH. The multicellular tumor spheroid model for high-throughput cancer drug discovery. Expert opinion on drug discovery. 2012; 7:819–30. [PubMed: 22788761]
6. Kunz-Schughart LA, Freyer JP, Hofstaedter F, et al. The use of 3-d cultures for high-throughput screening: The multicellular spheroid model. Journal of biomolecular screening. 2004; 9:273–85. [PubMed: 15191644]
7. Giacomotto J, Segalat L. High-throughput screening and small animal models, where are we? Br J Pharmacol. 2010; 160:204–16. [PubMed: 20423335]
8. Zon LI, Peterson RT. In vivo drug discovery in the zebrafish. Nat Rev Drug Discov. 2005; 4:35–44. [PubMed: 15688071]
9*. O'Reilly LP, Luke CJ, Perlmutter DH, et al. C. Elegans in high-throughput drug discovery. Adv Drug Deliv Rev. 2014; 69–70:247–53. Excellent review of the advantages and disadvantages of screening in *C. elegans*.
10. Breslin S, O'Driscoll L. Three-dimensional cell culture: The missing link in drug discovery. Drug discovery today. 2013; 18:240–9. [PubMed: 23073387]
11*. Swinney DC, Anthony J. How were new medicines discovered? Nat Rev Drug Discov. 2011; 10:507–19. Meta-analysis of how FDA-approved drugs were discovered, comparing phenotypic and target-based screening. [PubMed: 21701501]
12. Astashkina A, Grainger DW. Critical analysis of 3-d organoid in vitro cell culture models for high-throughput drug candidate toxicity assessments. Advanced drug delivery reviews. 2014; 69–70:1–18.
13. Rizvi I, Celli JP, Evans CL, et al. Synergistic enhancement of carboplatin efficacy with photodynamic therapy in a three-dimensional model for micrometastatic ovarian cancer. Cancer research. 2010; 70:9319–28. [PubMed: 21062986]
14. Montanez-Sauri SI, Beebe DJ, Sung KE. Microscale screening systems for 3d cellular microenvironments: Platforms, advances, and challenges. Cellular and molecular life sciences : CMLS. 2015; 72:237–49. [PubMed: 25274061]
15. Kimlin L, Kassis J, Virador V. 3d in vitro tissue models and their potential for drug screening. Expert opinion on drug discovery. 2013; 8:1455–66. [PubMed: 24144315]
16. Ranga A, Gjorevski N, Lutolf MP. Drug discovery through stem cell-based organoid models. Advanced drug delivery reviews. 2014; 69–70:19–28.
17. Nam KH, Smith AS, Lone S, et al. Biomimetic 3d tissue models for advanced high-throughput drug screening. Journal of laboratory automation. 2015; 20:201–15. [PubMed: 25385716]
18**. Vinci M, Gowan S, Boxall F, et al. Advances in establishment and analysis of three-dimensional tumor spheroid-based functional assays for target validation and drug evaluation. BMC biology. 2012; 10:29. Describes imaging-based 3D spheroid assays, including functional assays, for preclinical drug discovery. [PubMed: 22439642]
19. Soldatow VY, Lecluyse EL, Griffith LG, et al. Models for liver toxicity testing. Toxicol Res (Camb). 2013; 2:23–39. [PubMed: 23495363]

20. Rimann M, Laternser S, Gvozdenovic A, et al. An in vitro osteosarcoma 3d microtissue model for drug development. J Biotechnol. 2014; 189:129–35. [PubMed: 25234575]
21. Yoshii Y, Furukawa T, Waki A, et al. High-throughput screening with nanoimprinting 3d culture for efficient drug development by mimicking the tumor environment. Biomaterials. 2015; 51:278–89. [PubMed: 25771018]
22. ELB, Hsu YC, Lee JA. Consideration of the cellular microenvironment: Physiologically relevant co-culture systems in drug discovery. Advanced drug delivery reviews. 2014; 69–70:190–204.
23. Hoffmann OI, Ilmberger C, Magosch S, et al. Impact of the spheroid model complexity on drug response. Journal of biotechnology. 2015; 205:14–23. [PubMed: 25746901]
24. Kenny HA, Lal-Nag M, White EA, et al. Quantitative high throughput screening using a primary human three-dimensional organotypic culture predicts in vivo efficacy. Nature communications. 2015; 6:6220.
25. Lee JA, Chu S, Willard FS, et al. Open innovation for phenotypic drug discovery: The pd2 assay panel. Journal of biomolecular screening. 2011; 16:588–602. [PubMed: 21521801]
26. Ivanov DP, Parker TL, Walker DA, et al. Multiplexing spheroid volume, resazurin and acid phosphatase viability assays for high-throughput screening of tumour spheroids and stem cell neurospheres. PloS one. 2014; 9:e103817. [PubMed: 25119185]
27. Friedrich J, Seidel C, Ebner R, et al. Spheroid-based drug screen: Considerations and practical approach. Nature protocols. 2009; 4:309–24. [PubMed: 19214182]
28. Wenzel C, Riefke B, Grundemann S, et al. 3d high-content screening for the identification of compounds that target cells in dormant tumor spheroid regions. Experimental cell research. 2014; 323:131–43. [PubMed: 24480576]
29*. Ivascu A, Kubbies M. Rapid generation of single-tumor spheroids for high-throughput cell function and toxicity analysis. Journal of biomolecular screening. 2006; 11:922–32. Describes characterization of single-tumor spheroids and aggregates for multiple cell lines. [PubMed: 16973921]
30. Hongisto V, Jernstrom S, Fey V, et al. High-throughput 3d screening reveals differences in drug sensitivities between culture models of jimt1 breast cancer cells. PloS one. 2013; 8:e77232. [PubMed: 24194875]
31. Tung YC, Hsiao AY, Allen SG, et al. High-throughput 3d spheroid culture and drug testing using a 384 hanging drop array. The Analyst. 2011; 136:473–8. [PubMed: 20967331]
32. Hsiao AY, Tung YC, Qu X, et al. 384 hanging drop arrays give excellent z-factors and allow versatile formation of co-culture spheroids. Biotechnology and bioengineering. 2012; 109:1293–304. [PubMed: 22161651]
33. Cavnar SP, Salomonsson E, Luker KE, et al. Transfer, imaging, and analysis plate for facile handling of 384 hanging drop 3d tissue spheroids. Journal of laboratory automation. 2014; 19:208–14. [PubMed: 24051516]
34. Beauchamp P, Moritz W, Kelm JM, et al. Development and characterization of a scaffold-free 3d spheroid model of induced pluripotent stem cell-derived human cardiomyocytes. Tissue Eng Part C Methods. 2015
35. Timm DM, Chen J, Sing D, et al. A high-throughput three-dimensional cell migration assay for toxicity screening with mobile device-based macroscopic image analysis. Scientific reports. 2013; 3:3000. [PubMed: 24141454]
36. Guo WM, Loh XJ, Tan EY, et al. Development of a magnetic 3d spheroid platform with potential application for high-throughput drug screening. Molecular pharmaceutics. 2014; 11:2182–9. [PubMed: 24842574]
37. Ong SM, Zhao Z, Arooz T, et al. Engineering a scaffold-free 3d tumor model for in vitro drug penetration studies. Biomaterials. 2010; 31:1180–90. [PubMed: 19889455]
38. Thoma CR, Stroebel S, Rosch N, et al. A high-throughput-compatible 3d microtissue co-culture system for phenotypic rnai screening applications. Journal of biomolecular screening. 2013; 18:1330–7. [PubMed: 24080258]
39. Ivanov DP, Parker TL, Walker DA, et al. In vitro co-culture model of medulloblastoma and human neural stem cells for drug delivery assessment. Journal of biotechnology. 2015; 205:3–13. [PubMed: 25592050]

40. Howes AL, Richardson RD, Finlay D, et al. 3-dimensional culture systems for anti-cancer compound profiling and high-throughput screening reveal increases in egfr inhibitor-mediated cytotoxicity compared to monolayer culture systems. PloS one. 2014; 9:e108283. [PubMed: 25247711]
41. Li Q, Chen C, Kapadia A, et al. 3d models of epithelial-mesenchymal transition in breast cancer metastasis: High-throughput screening assay development, validation, and pilot screen. Journal of biomolecular screening. 2011; 16:141–54. [PubMed: 21297102]
42. Yoshii Y, Waki A, Yoshida K, et al. The use of nanoimprinted scaffolds as 3d culture models to facilitate spontaneous tumor cell migration and well-regulated spheroid formation. Biomaterials. 2011; 32:6052–8. [PubMed: 21640378]
43. Cho CH, Park J, Tilles AW, et al. Layered patterning of hepatocytes in co-culture systems using microfabricated stencils. Biotechniques. 2010; 48:47–52. [PubMed: 20078427]
44. No da Y, Lee SA, Choi YY, et al. Functional 3d human primary hepatocyte spheroids made by co-culturing hepatocytes from partial hepatectomy specimens and human adipose-derived stem cells. PLoS One. 2012; 7:e50723. [PubMed: 23236387]
45. Krausz E, de Hoogt R, Gustin E, et al. Translation of a tumor microenvironment mimicking 3d tumor growth co-culture assay platform to high-content screening. Journal of biomolecular screening. 2013; 18:54–66. [PubMed: 22923784]
46. Anderson SN, Towne DL, Burns DJ, et al. A high-throughput soft agar assay for identification of anticancer compound. Journal of biomolecular screening. 2007; 12:938–45. [PubMed: 17942786]
47. Lovitt CJ, Shelper TB, Avery VM. Miniaturized three-dimensional cancer model for drug evaluation. Assay and drug development technologies. 2013; 11:435–48. [PubMed: 25310845]
48. Horman SR, To J, Orth AP. An hts-compatible 3d colony formation assay to identify tumor-specific chemotherapeutics. Journal of biomolecular screening. 2013; 18:1298–308. [PubMed: 23918920]
49. Rimann M, Angres B, Patocchi-Tenzer I, et al. Automation of 3d cell culture using chemically defined hydrogels. Journal of laboratory automation. 2014; 19:191–7. [PubMed: 24132162]
50. Godugu C, Patel AR, Desai U, et al. Algimatrix based 3d cell culture system as an in-vitro tumor model for anticancer studies. PloS one. 2013; 8:e53708. [PubMed: 23349734]
51. Zhang X, Wang W, Yu W, et al. Development of an in vitro multicellular tumor spheroid model using microencapsulation and its application in anticancer drug screening and testing. Biotechnology progress. 2005; 21:1289–96. [PubMed: 16080713]
52. Reid BG, Jerjian T, Patel P, et al. Live multicellular tumor spheroid models for high-content imaging and screening in cancer drug discovery. Current chemical genomics and translational medicine. 2014; 8:27–35. [PubMed: 24596682]
53*. Letamendia A, Quevedo C, Ibarbia I, et al. Development and validation of an automated high-throughput system for zebrafish in vivo screenings. PLoS One. 2012; 7:e36690. Zebrafish high-throughput screen for angiogenesis and cardiotoxicity, using automated sorter for animal dispensing and liquid handlers for compound addition and embryo immobilization. [PubMed: 22615792]
54. Milan DJ. Drugs that induce repolarization abnormalities cause bradycardia in zebrafish. Circulation. 2003; 107:1355–8. [PubMed: 12642353]
55. Rihel J, Prober DA, Arvanites A, et al. Zebrafish behavioral profiling links drugs to biological targets and rest/wake regulation. Science. 2010; 327:348–51. [PubMed: 20075256]
56. Pardo-Martin C, Chang TY, Koo BK, et al. High-throughput in vivo vertebrate screening. Nat Methods. 2010; 7:634–6. [PubMed: 20639868]
57. Vogt A, Cholewinski A, Shen X, et al. Automated image-based phenotypic analysis in zebrafish embryos. Dev Dyn. 2009; 238:656–63. [PubMed: 19235725]
58. Peravali R, Gehrig J, Giselbrecht S, et al. Automated feature detection and imaging for high-resolution screening of zebrafish embryos. Biotechniques. 2011; 50:319–24. [PubMed: 21548893]
59. Gehrig J, Reischl M, Kalmar E, et al. Automated high-throughput mapping of promoter-enhancer interactions in zebrafish embryos. Nat Methods. 2009; 6:911–6. [PubMed: 19898487]
60. Corsi AK, Wightman B, Chalfie M. A transparent window into biology: A primer on caenorhabditis elegans. Genetics. 2015; 200:387–407. [PubMed: 26088431]

61**. Gosai SJ, Kwak JH, Luke CJ, et al. Automated high-content live animal drug screening using c. Elegans expressing the aggregation prone serpin alpha1-antitrypsin z. PLoS One. 2010; 5:e15460. High-throughput screen in *C. elegans* using automated animal sorting and dedicated high content imaging instrument, with a multiplex readout based on live/dead staining in fluorescent transgenic line. [PubMed: 21103396]

62. Leung CK, Deonarine A, Strange K, et al. High-throughput screening and biosensing with fluorescent c. Elegans strains. J Vis Exp. 2011

63. Leung CK, Wang Y, Malany S, et al. An ultra high-throughput, whole-animal screen for small molecule modulators of a specific genetic pathway in caenorhabditis elegans. PLoS One. 2013; 8:e62166. [PubMed: 23637990]

64. Moy TI, Conery AL, Larkins-Ford J, et al. High-throughput screen for novel antimicrobials using a whole animal infection model. ACS Chem Biol. 2009; 4:527–33. [PubMed: 19572548]

65*. Giepmans BN, Adams SR, Ellisman MH, et al. The fluorescent toolbox for assessing protein location and function. Science. 2006; 312:217–24. This article reviews fluorescent sensors. [PubMed: 16614209]

66. Klein OJ, Bhayana B, Park YJ, et al. In vitro optimization of etnbs-pdt against hypoxic tumor environments with a tiered, high-content, 3d model optical screening platform. Molecular pharmaceutics. 2012; 9:3171–82. [PubMed: 22946843]

67. Vamvakidou AP, Mondrinos MJ, Petushi SP, et al. Heterogeneous breast tumoroids: An in vitro assay for investigating cellular heterogeneity and drug delivery. Journal of biomolecular screening. 2007; 12:13–20. [PubMed: 17166827]

68. Wittig R, Richter V, Wittig-Blaich S, et al. Biosensor-expressing spheroid cultures for imaging of drug-induced effects in three dimensions. J Biomol Screen. 2013; 18:736–43. [PubMed: 23479354]

69. Lin S, Zhao Y, Xia T, et al. High content screening in zebrafish speeds up hazard ranking of transition metal oxide nanoparticles. ACS Nano. 2011; 5:7284–95. [PubMed: 21851096]

70. Gallardo VE, Varshney GK, Lee M, et al. Phenotype-driven chemical screening in zebrafish for compounds that inhibit collective cell migration identifies multiple pathways potentially involved in metastatic invasion. Dis Model Mech. 2015; 8:565–76. [PubMed: 25810455]

71. Tsuji Y, Takahashi N, Fletcher JG, et al. Subtraction color map of contrast-enhanced and unenhanced ct for the prediction of pancreatic necrosis in early stage of acute pancreatitis. AJR Am J Roentgenol. 2014; 202:W349–56. [PubMed: 24660733]

72. Tsuji N, Ninov N, Delawary M, et al. Whole organism high content screening identifies stimulators of pancreatic beta-cell proliferation. PLoS One. 2014; 9:e104112. [PubMed: 25117518]

73. Maglioni S, Arsalan N, Franchi L, et al. An automated phenotype-based microscopy screen to identify pro-longevity interventions acting through mitochondria in c. Elegans. Biochim Biophys Acta. 2015

74. Kerr RA. Imaging the activity of neurons and muscles. WormBook. 2006:1–13. [PubMed: 18050440]

75. https://www.microscopyu.com/articles/formulas/formulasfielddepth.html

76. Godin AG, Lounis B, Cognet L. Super-resolution microscopy approaches for live cell imaging. Biophys J. 2014; 107:1777–84. [PubMed: 25418158]

77. Lee MK, Rai P, Williams J, et al. Small-molecule labeling of live cell surfaces for three-dimensional super-resolution microscopy. J Am Chem Soc. 2014; 136:14003–6. [PubMed: 25222297]

78. Winter PW, Chandris P, Fischer RS, et al. Incoherent structured illumination improves optical sectioning and contrast in multiphoton super-resolution microscopy. Opt Express. 2015; 23:5327–34. [PubMed: 25836564]

79. Chen BC, Legant WR, Wang K, et al. Lattice light-sheet microscopy: Imaging molecules to embryos at high spatiotemporal resolution. Science. 2014; 346:1257998. [PubMed: 25342811]

80*. Pampaloni F, Ansari N, Stelzer EH. High-resolution deep imaging of live cellular spheroids with light-sheet-based fluorescence microscopy. Cell Tissue Res. 2013; 352:161–77. Compares

imaging of spheroids using confocal imaging and light sheet based fluorescence microscopy. [PubMed: 23443300]

81. Konig K, Uchugonova A, Gorjup E. Multiphoton fluorescence lifetime imaging of 3d-stem cell spheroids during differentiation. Microsc Res Tech. 2011; 74:9–17. [PubMed: 21181704]
82*. Swedlow JR. Quantitative fluorescence microscopy and image deconvolution. Methods Cell Biol. 2013; 114:407–26. Review discusses fluorescence microscopy and imaging. [PubMed: 23931516]
83*. Schermelleh L, Heintzmann R, Leonhardt H. A guide to super-resolution fluorescence microscopy. J Cell Biol. 2010; 190:165–75. Review discusses super-resolution imaging technologies. [PubMed: 20643879]
84. Schindelin J, Arganda-Carreras I, Frise E, et al. Fiji: An open-source platform for biological-image analysis. Nat Methods. 2012; 9:676–82. [PubMed: 22743772]
85. Carpenter AE, Jones TR, Lamprecht MR, et al. Cellprofiler: Image analysis software for identifying and quantifying cell phenotypes. Genome Biol. 2006; 7:R100. [PubMed: 17076895]
86. Cornelissen F, Cik M, Gustin E. Phaedra, a protocol-driven system for analysis and validation of high-content imaging and flow cytometry. J Biomol Screen. 2012; 17:496–506. [PubMed: 22233649]
87. Linkert M, Rueden CT, Allan C, et al. Metadata matters: Access to image data in the real world. J Cell Biol. 2010; 189:777–82. [PubMed: 20513764]
88. Goldberg IG, Allan C, Burel JM, et al. The open microscopy environment (ome) data model and xml file: Open tools for informatics and quantitative analysis in biological imaging. Genome Biol. 2005; 6:R47. [PubMed: 15892875]
89. Allan C, Burel JM, Moore J, et al. Omero: Flexible, model-driven data management for experimental biology. Nat Methods. 2012; 9:245–53. [PubMed: 22373911]
90. Di Z, Klop MJ, Rogkoti VM, et al. Ultra high content image analysis and phenotype profiling of 3d cultured micro-tissues. PLoS One. 2014; 9:e109688. [PubMed: 25289886]
91. Ollion J, Cochennec J, Loll F, et al. Tango: A generic tool for high-throughput 3d image analysis for studying nuclear organization. Bioinformatics. 2013; 29:1840–1. [PubMed: 23681123]
92. Bilgin CC, Kim S, Leung E, et al. Integrated profiling of three dimensional cell culture models and 3d microscopy. Bioinformatics. 2013; 29:3087–93. [PubMed: 24045773]
93. Peng H, Ruan Z, Long F, et al. V3d enables real-time 3d visualization and quantitative analysis of large-scale biological image data sets. Nat Biotechnol. 2010; 28:348–53. [PubMed: 20231818]
94. Bonnier F, Keating ME, Wrobel TP, et al. Cell viability assessment using the alamar blue assay: A comparison of 2d and 3d cell culture models. Toxicol In Vitro. 2015; 29:124–31. [PubMed: 25300790]
95. Oshikata A, Matsushita T, Ueoka R. Enhancement of drug efflux activity via mdr1 protein by spheroid culture of human hepatic cancer cells. J Biosci Bioeng. 2011; 111:590–3. [PubMed: 21354366]
96. Nichols AJ, Roussakis E, Klein OJ, et al. Click-assembled, oxygen-sensing nanoconjugates for depth-resolved, near-infrared imaging in a 3d cancer model. Angew Chem Int Ed Engl. 2014; 53:3671–4. [PubMed: 24590700]
97. Erturk A, Bradke F. High-resolution imaging of entire organs by 3-dimensional imaging of solvent cleared organs (3disco). Experimental neurology. 2013; 242:57–64. [PubMed: 23124097]
98. Hama H, Kurokawa H, Kawano H, et al. Scale: A chemical approach for fluorescence imaging and reconstruction of transparent mouse brain. Nature neuroscience. 2011; 14:1481–8. [PubMed: 21878933]
99. Chung K, Wallace J, Kim SY, et al. Structural and molecular interrogation of intact biological systems. Nature. 2013; 497:332–7. [PubMed: 23575631]
100*. Boutin ME, Hoffman-Kim D. Application and assessment of optical clearing methods for imaging of tissue-engineered neural stem cell spheres. Tissue Eng Part C Methods. 2015; 21:292–302. Application of multiple optical clearing protocols for the imaging of scaffold-free spheroids. [PubMed: 25128373]

Article Highlights

- The increased interest in phenotypic screening coupled with evidence showing cells grown in three dimensional structures more closely recapitulate *in vivo* drug response makes high throughput, 3D fluorescent imaging screens an attractive option for drug discovery.
- There are many methods in use for making both single and multi-cell type spheroids, both of which display differential properties for ease of culture and drug sensitivities.
- Whole animal screening is primarily done in *C. elegans* or *D. rerio* due to their optical transparency and relative ease of husbandry, but achieving true high throughput still poses technical challenges.
- Fluorescent sensors must be adapted for 3D culture, especially due to variable dye penetration in thick spheroids or through animal tissues, or the effort must be made to create stable transgenic lines.
- Recent advances in microscopy have made high speed-high content imaging more attainable, but physical properties like sample thickness or light scattering necessitate different technologies for 3D imaging as compared to traditional monolayers.
- Most current software systems capable of handling typical screening datasets primarily modify 2D analysis techniques for 3D images, such as maximum projections from Z-stacks, with only a few truly 3D options available.

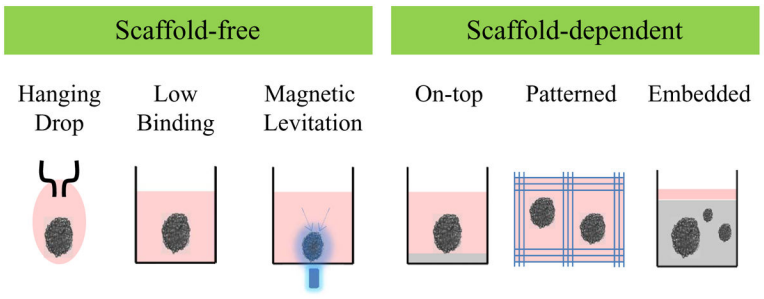

Figure 1.
Schematic representation of most common scaffold-free and scaffold-independent 3D cellular culturing methods amenable for high-throughput assays.

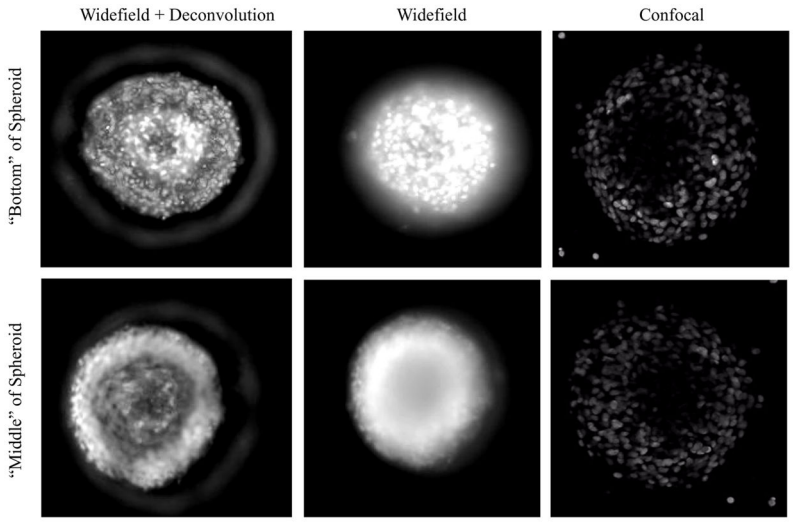

Figure 2.

3D rendering of Z stacks using current microscopy methods. Spheroids of Panc-1 cells were generated in 384-well ULA plates (Corning) at 37 °C, 5% CO_2, 95% RH for 7 days. Spheroids were stained with 10 μg/ml Hoechst 33342 for 60 minutes prior to imaging. Widefield images were captured on an IN Cell 2000 High Content Imaging system at 20X (0.70 NA) with 13 Z sections at 5 μm per section. Image volumes were rendered using FIJI and the ImageJ 3D viewer plugin and standard rendering settings. Identically spaced sections were captured on a Zeiss LSM 710 Confocal point scanning confocal microscope using a 20x 0.8 NA air objective and a 3 micron pinhole. Representative "bottom" (closest to well bottom) and "middle" image snapshots are displayed. Deconvolution of image stacks was conducted using the IN Cell 3D deconvolution software (Enhanced Ratio Aggressive Deconvolution method with 10 cycles).

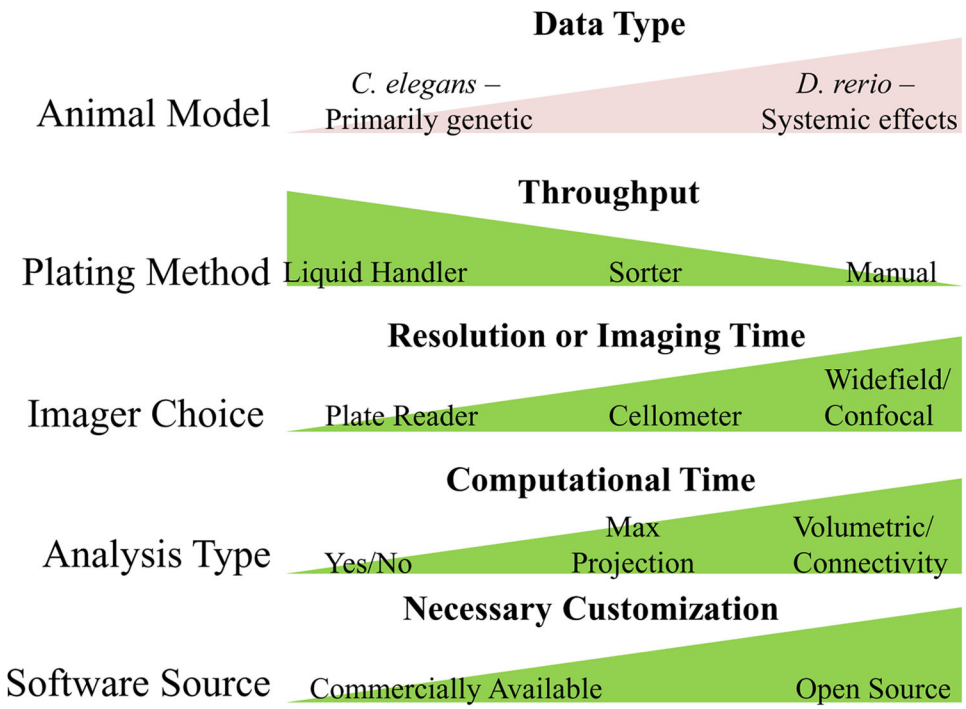

Figure 3.

Many factors must be taken into account when designing a 3D screen and desired readout. For each step, the primary consideration is in bold. However, each of these are generally directly related to the other considerations listed (i.e. as resolution increases, so does computational time). Throughput is the exception, in that it is usually inversely correlated with the other parameters as listed. For the animal models, we tried to reflect necessary prior knowledge and the types of data generally returned. *C. elegans* is typically best suited to drug screens geared towards diseases or compounds with well understood targets known to have orthologs in worms. *D. rerio* develops organ systems more similar to mammals and can therefore more readily be used to assess systemic effects (i.e. cardiovascular toxicities or developmental defects).

Table 1

3D cellular culture methods

Scaffold	Method	Throughput	Advantages	Limitations	Commercial Plate
Free (liquid overlay)	ULA plate	96 and 384	Uniform size, single spheroids/well. Simple protocol	Not amenable to media changes. Not suitable to all cell types. Autofocus issues	Corning, PerkinElmer
	Agarose-coated plate	96 and 384	Uniform size, single spheroids/well	Not amenable to media changes. Not suitable to all cell types. Autofocus issues	
	poly-HEMA-coated plate	96 and 384	Single spheroids/well	Not amenable to media changes. Not suitable to all cell types. Spheroids not uniform in size. Autofocus issues	
	Hanging drop	96 and 384	Uniform size, single spheroids/well	Requires transfer of spheroids to other plates. Not amenable to media changes. Autofocus issues	InSphero, 3D Biomatrix
	Magnetic levitation	96	Uniform size, single spheroids/well. Amenable to media changes	Unknown effect of magnetic nanoparticles on cellular responses. Requires magnetic plate adapters	Nano3D
On-top	Natural ECM layer	96 and 384	Compact spheroid formation. Suitable to all cell types. Biologically relevant interactions	ECM suffers from batch variations. Possible optical aberrations	
	Micro-patterned plates	96	Uniform size spheroid arrays	Uneven distribution of spheroids. Requires modest investment in cell growth optimization. Possible optical aberrations	Cytoo, Toyo Gosei, Scivax
Embedded	Natural ECM	96 and 384	Compact spheroid formation. Suitable to all cell types. Biologically relevant interactions	Difficult to control spheroid size and number/well. *In situ* imaging is limited and prior removal of scaffold might be required. Natural ECM suffers from batch variations	
	Agar	96 and 384	Compact spheroid formation. Suitable to all cell types	Difficult to control spheroid size and number/well. In situ imaging is limited and prior removal of scaffold might be required	
	Hydrogel /Alginate		Compact spheroid formation. Suitable to all cell types. Allows modulation of scaffold stiffness	Difficult to control spheroid size and number/well. In situ imaging is limited and prior removal of scaffold might be required	Cellendes, Pancea, Sigma

Expert Opin Drug Discov. Author manuscript; available in PMC 2016 December 01.

Table 2

Fluorescence Imaging Technologies

Microscopy	Advantages	Limitations	Examples
Confocal	Background light rejection (autofluorescence and image sectioning)	Costly, can reduce light at sample	Spinning Disc, Point scanning, Laser Line
Widefield	Low cost, fast	Does not reduce background	SSI, Metal Halide excitation
Widefield + Deconvolution	Increased contrast and resolution, can reduce background under certain circumstances	Not always quantitative, processing can be slow, image artifacts	Deconvolution algorithms (nearest neighbor, constrained iterative, etc.)
Super Resolution	Detect subcellular localization, possibly deeper penetration	Low throughput, typically 1 or less spheroid/image	TIRF, SIM, STED

Table 3

Imaging Platforms

Platform	Advantages	Limitations	Examples
Whole well imagers	Low cost, fast, easy to use	Resolution limited	Nexcelom; Celigo, Pekin Elmer; EnSight, Nano3D
Fluorescence Microscopes	Subcellular resolution	May require additional modules (autofocus, Z motors, stage). Can be difficult to set up and use in an automated environment	Many (Zeiss, Olympus, Nikon, etc)
HCA Systems	Fast, subcellular resolution, “out of the box” solution	Can be costly and difficult to use	GE: IN Cell, MD: IMageXpress, Life: Arrayscan, PE: Operetta, Phenix, TTP; Acumen, Idea Bio; Wiscan, Vala; IC - Series, Wako; Cellvoyager, Essen; Incucyte